New Evidence on the State of Stress of the San Andreas Fault System

MARK D. ZOBACK, MARY LOU ZOBACK, VAN S. MOUNT, JOHN SUPPE, JERRY P. EATON, JOHN H. HEALY, DAVID OPPENHEIMER, PAUL REASENBERG, LUCILE JONES, C. BARRY RALEIGH, IVAN G. WONG, OONA SCOTTI, CARL WENTWORTH

Contemporary in situ tectonic stress indicators along the San Andreas fault system in central California show northeast-directed horizontal compression that is nearly perpendicular to the strike of the fault. Such compression explains recent uplift of the Coast Ranges and the numerous active reverse faults and folds that trend nearly parallel to the San Andreas and that are otherwise unexplainable in terms of strike-slip deformation. Fault-normal crustal compression in central California is proposed to result from the extremely low shear strength of the San Andreas and the slightly convergent relative motion between the Pacific and North American plates. Preliminary in situ stress data from the Cajon Pass scientific drill hole (located 3.6 kilometers northeast of the San Andreas in southern California near San Bernardino, California) are also consistent with a weak fault, as they show no right-lateral shear stress at ~2-kilometer depth on planes parallel to the San Andreas fault.

FOR ALMOST 20 YEARS, A FUNDAMENTAL PARADOX HAS existed about the level of shear stress required to cause motion along major plate-bounding faults like the San Andreas. This paradox, often referred to as the stress–heat flow paradox, arises from the fact that over a hundred observations of conductive heat flow in shallow boreholes near the San Andreas have detected no evidence of frictionally generated heat, implying that the fault slips at extremely low average shear stresses on the order of 10 to 20 mega/pascals (MPa) (*1–3*). Although such stresses are on the order of the seismic stress drops of earthquakes (*4*), they are a factor of 5 to 10 less than the average shear stress predicted by frictional faulting theory from laboratory-derived values of rock friction (*5–8*). As the much higher stress levels predicted by faulting theory and laboratory data are consistent with estimated shear stress levels required to support topography and explain lithospheric flexure (*9*), such levels are widely used as a fundamental constraint for stresses in the upper crust in theoretical studies of lithospheric deformation and flexure (*10*). Moreover, frictional slip between rock samples in the laboratory is widely used as an analog for brittle faulting in the upper 15 to 20 km of the crust (*11*). An understanding of the basic physical mechanisms that control motion along major plate boundaries, the balance of the forces that cause and resist plate motion, and the overall boundary conditions that control deformation along plate boundaries and within the plates, require resolution of this issue.

Although in situ stress measurements near the San Andreas and other faults are generally consistent with classical faulting theory and laboratory-derived friction values (*12*), the measurements are at relatively shallow depths (<0.9 km) and are difficult to extrapolate to the upper 15 to 20 km of the crust. Also, the shallow conductive heat flow measurements (most of the data come from boreholes that are only ~300 m deep) may be contaminated by near-surface thermal convection, which would obviate their significance (*13*). Although arguments have been made that significant convective heat flow is not occurring near the fault (*3*) the debate about the level of shear stress on the fault has continued (*14*). To help resolve this paradox, continental scientific drilling is currently under way at a site 3.5 km from the San Andreas fault at Cajon Pass, California, with the goal of measuring in situ stress and heat flow at seismogenic depth (*15*).

There is considerable data indicating that the San Andreas is essentially a pure right-lateral strike-slip transform fault with hundreds of kilometers of displacement along it. However, since the advent of plate tectonics theory in the mid-1960s, a long-standing geological question is how to account for the widespread occurrence of folds and reverse faults that roughly parallel the San Andreas and indicate compression nearly orthogonal to the fault. In terms of classical faulting theory (*6, 7*), the direction of maximum horizontal compression is expected to be 30° to 45° from a vertical strike-slip fault plane. If so, the stress fields associated with right-lateral strike-slip motion on the northwest-trending, near vertical San Andreas and dip-slip motion on nearly parallel reverse faults would be completely incompatible.

These two fundamental problems of San Andreas tectonics, the stress–heat flow paradox and the origin of near fault-parallel folding and reverse faulting, have a common explanation. We demonstrate that the direction of maximum horizontal compression in western California is not an angle of about 30° to 40° to the strike of San Andreas fault, as expected from frictional faulting theory, but is oriented nearly orthogonal to the strike of the fault. We suggest that although stresses in the lithosphere are generally high, the cause of

M. D. Zoback and O. Scotti are in the Department of Geophysics, Stanford University, Stanford, CA 94305. M. L. Zoback, J. P. Eaton, J. H. Healy, D. Oppenheimer, P. Reasenberg, and C. Wentworth are at the U.S. Geological Survey, Menlo Park, CA 94025. V. S. Mount and J. Suppe are in the Department of Geology and Geophysical Sciences, Princeton University, Princeton, NJ 08544. L. Jones is at the U.S. Geological Survey, Pasadena, CA 91107. C. B. Raleigh is at the Lamont-Doherty Geological Observatory, Columbia University, Palisades, NY 10964. I. G. Wong is at Woodward-Clyde Consultants, San Francisco, CA 94102.

the fault-normal stress field near the San Andreas is an extremely weak fault (as implied by the heat flow data) that nearly totally relieves shear stresses parallel to the fault (*16*). Because relative motion of the Pacific and North American plates is slightly convergent, the component of convergent plate motion normal to the San Andreas is accommodated through folding and reverse faulting on structures that are subparallel to the San Andreas, which is consistent with the orientation of the local stress field. We first present evidence establishing the current state of stress along the San Andreas fault system and the nature of geologic deformation in the region adjacent to the fault in the last 4 to 5 million years. We then interpret these data in terms of a model of the San Andreas fault that is consistent with both low shear-stress levels on the fault and generally high shear stresses in the lithosphere, as well as relative plate motions. Finally, we briefly discuss the implications of these data with respect to the constitutive properties of a weak fault zone.

State of stress in central California. Figure 1 presents about 200 quality-ranked measurements of the orientation of the maximum principal tectonic stress in California. The data are from stress-induced wellbore breakouts, earthquake focal plane mechanisms, hydraulic fracturing in situ stress measurements, and young (<2 million years old) volcanic alignments. We do not include in Fig. 1 right-lateral strike-slip focal mechanisms along the San Andreas fault, or the other major subparallel strike-slip faults (for example, the Hayward, Calaveras, and San Jacinto faults). Instead, we simply show with arrows the sense of lateral movement on these faults as inferred from the focal mechanisms, fault creep in central California, and co-seismic fault offsets. The criteria used in the evaluation of tectonic stress indicators and the quality-ranking of the data in the compilation have been described (*17*). In general, focal mechanism data used in this compilation have been restricted to earthquakes that have occurred in the past decade because of the greatly improved seismographic coverage since the late 1970s. When possible, we also prefer to consider the average of several focal mechanisms in a given area to determine the direction of maximum horizontal compression (*18*). In situ stress measurements are includ-

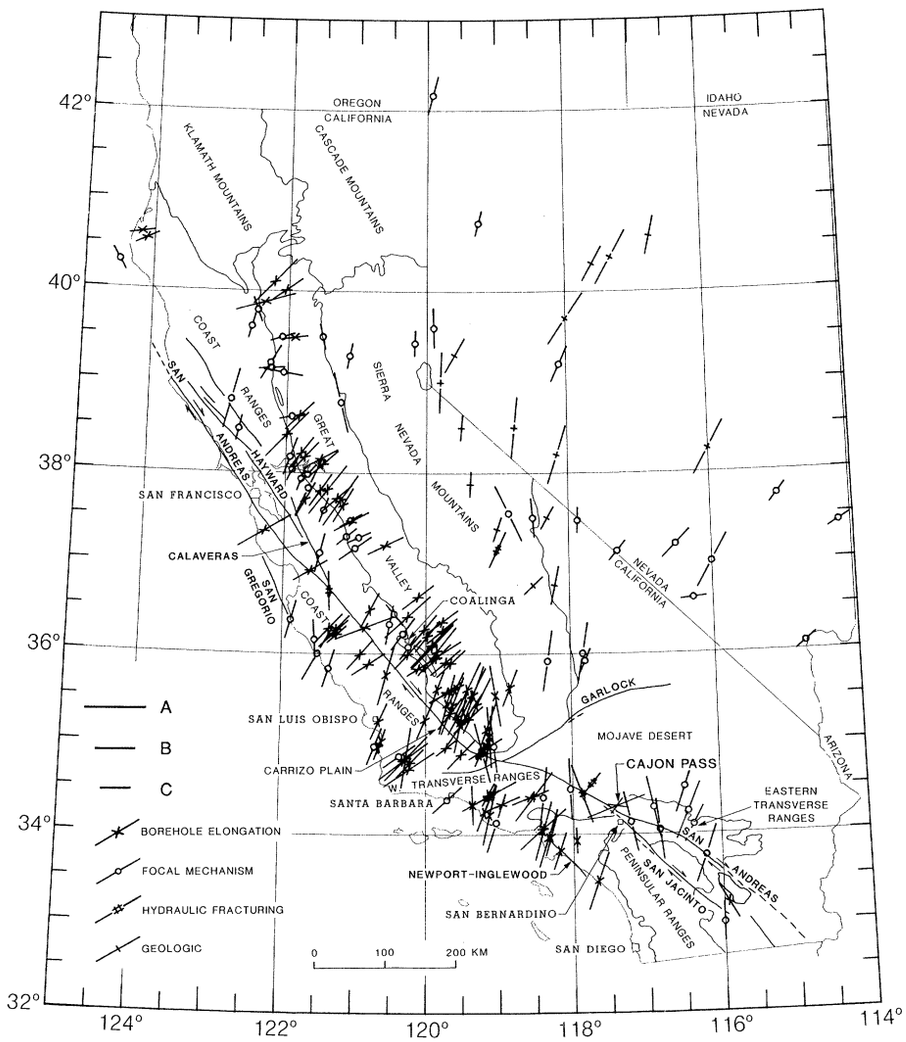

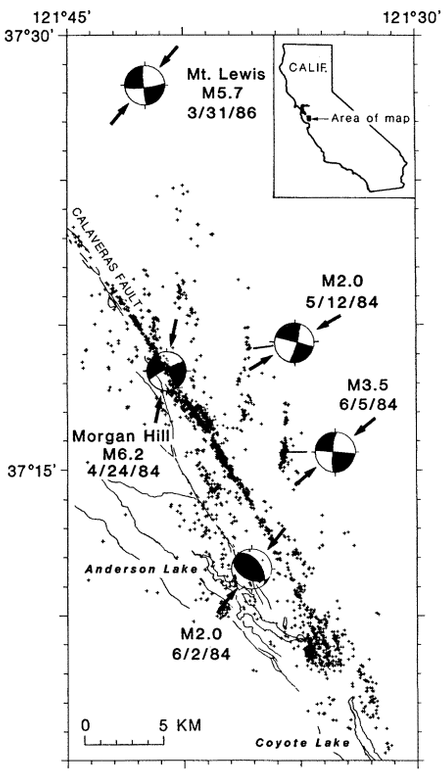

Fig. 1 (left). Generalized geologic map of California with data points showing the direction of maximum horizontal compression in the crust. The length of the bars attached to each data point is a measure of its quality (A, B, or C). The symbol associated with each data point indicates the type of stress indicator. No focal mechanisms from earthquakes directly on the San Andreas or major, right-lateral strike-slip subsidiary faults are included.

Fig. 2 (right). Earthquakes and focal mechanisms in the vicinity of the 1984 Morgan Hill earthquake on the Calaveras fault. Aftershock epicenters (shown as crosses) delineate the main rupture on the Calaveras fault as well as abundant off-fault seismicity. The main shock was a right-lateral strike-slip event on the Calaveras. Off-fault events occurring both before and after the main shock (represented by characteristic focal mechanisms) show fault-normal compression immediately east and west of the main fault trace. The Mount Lewis earthquake focal mechanism also shows maximum compression almost perpendicular to the Calaveras.

ed only from depths greater than 100 m in order to filter out data contaminated by nontectonic sources of stress that are often prevalent at extremely shallow depth (*19*). An important component of the stress map that accounts for about half of the data points in west-central California is stress-induced wellbore breakouts (*20*). These data are from depths of 1 to 4 km, the depth range of petroleum wells in the region. The use of stress-induced breakouts for in situ stress determination is well established (*21*).

At the many locations where different types of stress indicators are present, there is a good correlation between the different types of stress data (see especially the correlation between focal mechanisms and borehole elongation in central California), which indicates that (i) the criteria used for evaluation of the different types of data as indicators of tectonic stress are approximately correct and (ii) there is no indication that the direction of maximum compression changes between the upper 4 km (the source of the borehole data) and the midcrust (4 to 15 km) (the source of most of the earthquake focal mechanism data).

At least two major stress provinces are clearly defined north of the Garlock fault. In the eastern part of the state [east of the Great Central Valley (Fig. 1)], there is significant evidence of both strike-slip and extensional faulting. This style of deformation, along with the approximately east-west direction of extension, suggests that the tectonics of eastern California are transitional between the Basin and Range province further to the east and the San Andreas province to the west (*17, 22*). In western California, however, the style of deformation in the San Andreas province is compressional and dominated by strike-slip and reverse faulting. Clearly, the most striking feature of the stress map is that the direction of maximum horizontal compression in central California is nearly perpendicular to the San Andreas fault.

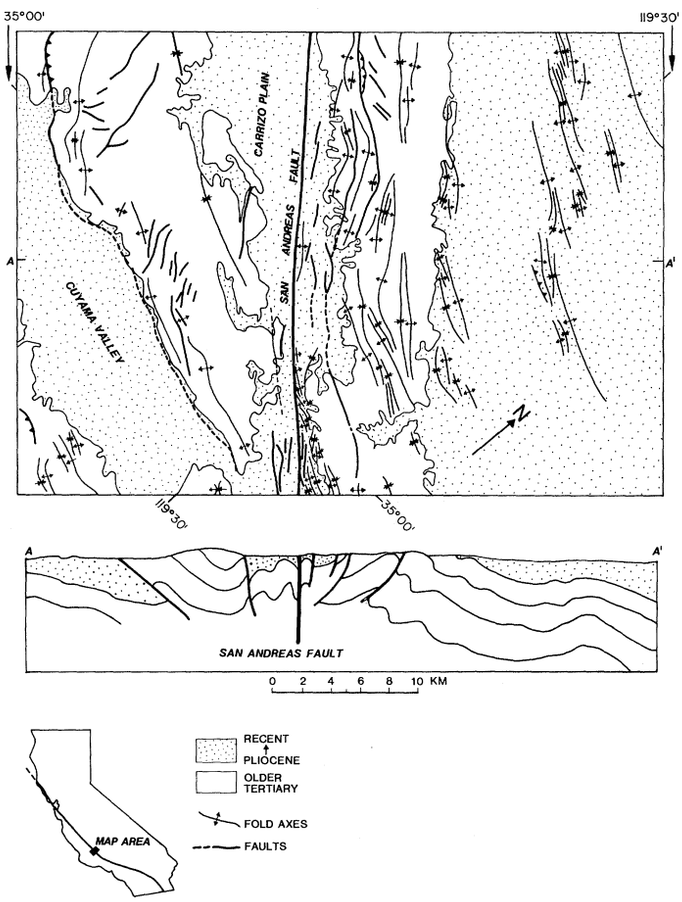

Fig. 3. Geologic map and cross section of active faults and folds in the Carrizo Plain area, which show evidence for active compression perpendicular to the San Andreas fault (*32*).

Other evidence of fault-normal compression in central California. There are many geologic indicators of fault-normal compressional deformation in the vicinity of the San Andreas fault that can be shown to be younger than 4 to 5 million years old. This time period is important for two reasons. First, the triple junction that migrates northward along the San Andreas was north of San Francisco 5 million years ago and the tectonics of the region to the south would presumably be dominated strictly by the strike-slip tectonics that are active today (*23*). Second, a significant clockwise change in the absolute Pacific plate motion seems to have occurred about 4 to 5 million years ago (*24*), which produces a component of convergence in North America–Pacific relative plate motion that may be ultimately responsible for the observed fault-normal compression.

Perhaps the most dramatic example of geologically recent fault-normal compression is uplift of the Coast Ranges. Subprovinces of the Coast Ranges, such as the Santa Cruz, Santa Lucia, Diablo, Gabilan, and Temblor ranges, and the adjacent alluviated depressions (Santa Clara valley, Salinas valley, and Carrizo plain), all strike subparallel to the San Andreas. Uplift of these ranges cannot be explained in terms of the strike-slip faulting associated with the fault (*25*). Numerous occurrences of deformed Plio-Pleistocene (and younger) strata document the ongoing uplift and internal deformation of the Coast Ranges in a manner consistent with compressive stresses oriented approximately orthogonal to the San Andreas fault (*25*).

Currently active reverse faulting and folding along nearly the entire length of the west side of the Great Central Valley are another large-scale example of compression essentially perpendicular to the San Andreas fault (*26*). Focal mechanisms of the recent Coalinga (1983, magnitude $M = 6.7$) and North Kettleman Hills (1985, $M = 5.7$) earthquakes indicate compression essentially orthogonal to the San Andreas fault (*27, 28*). Similar earthquake focal mechanisms are observed along much of the west side of the valley.

Smaller scale examples of active fault-normal compression include northwest trending Plio-Pleistocene folds and high-angle reverse faults in the Santa Lucia range, en echelon Plio-Pleistocene folds west of Salinas valley and the Rinconada fault, and the large number of northwest-trending Neogene folds in the section of the state roughly bounded by Santa Barbara, San Luis Obispo, Coalinga, and the Carrizo plain (*25*). Numerous examples of Pliocene and younger reverse faults in the southern San Francisco Bay area indicate northeast compression, essentially perpendicular to the San Andreas (*29*). Numerous features offshore central California suggest that similar deformation is occurring off the coast (*30*), and a recent statistical analysis of Pliocene and younger geologic structures in coastal central California indicates that the direction of maximum principal stress is about N33°E (*31*).

Specific examples of fault-normal compression within just a few kilometers of the San Andreas and Calaveras faults are shown in Figs. 2 and 3. Figure 2 shows the recent seismicity in the area of the Morgan Hill (1984, $M = 6.2$) earthquake that occurred along the Calaveras fault. A detailed map and cross section in the Carrizo Plain area (Fig. 3) shows intensive folding adjacent to the San Andreas in the past 4 million years that results from fault-normal compression (*32*). The main-shock focal mechanism of the Morgan Hill earthquake shows right-lateral strike-slip motion on a vertical fault. Off-fault earthquakes, however, indicate a markedly different style of deformation, one clearly associated with northeast-oriented compression approximately perpendicular to the strike of the Calaveras. East of the fault, the focal mechanism and aftershock pattern of the

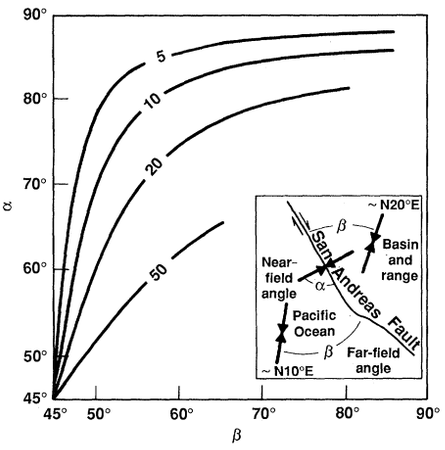

Fig. 4. Angle between the San Andreas fault and the maximum principal stress near the fault as a function of the orientation of the far-field maximum principal stress for different values of fault strength in megapascals (*50, 51*).

Mount Lewis (1986, M = 5.7) earthquake, as well as focal mechanisms and hypocentral distribution of aftershocks of the Morgan Hill event, show right-lateral strike-slip motion on north-striking vertical faults and northeast-directed P-axes. West of the Calaveras, earthquakes that occurred in the Anderson Lake area prior to the Morgan Hill earthquake show reverse faulting on planes parallel to the Calaveras. In both of these cases (Figs. 2 and 3), near fault-normal compression is observed within only a few kilometers of the major right-lateral strike-slip fault.

There are several other indications of fault-normal compression in recent seismicity. Focal mechanisms throughout the Coast Ranges in central California generally indicate northeasterly compressive stress (*33*). In the Bear valley area of central California (~30 km southeast of the intersection of the San Andreas and Calaveras faults), earthquake focal mechanisms directly on the fault are consistent with northwest-striking right-lateral strike-slip fault, whereas those immediately off the fault show northeast compression that is nearly perpendicular to the fault (*34*).

Because of the high rate (~25 to 35 mm/year) of ongoing right-lateral strike-slip movement along the San Andreas (and related faults) at depths beneath the seismogenic upper crust, geodetic networks that straddle these faults show deformation consistent with such horizontal shear (*35*). However, it would be difficult to detect a few millimeters per year of fault-normal crustal shortening through analysis of the strain occurring within these networks. Moreover, inversion of the geodetic data for displacements along the fault is typically done with boundary conditions that minimize fault-normal displacements (*36*). Thus these analyses would not normally detect fault-normal movement. However, several studies of geodetic data in central California have revealed some indication of compression oriented highly obliquely to the trend of the fault (*37*). Unfortunately, these studies rely on somewhat old geodetic data in which it is difficult to ascertain the significance of possible systematic errors.

We propose that the orientation of the tectonic stress field shown in Figs. 1 to 3 demonstrates that the resolved shear stresses on the San Andreas fault are extremely low, as implied by heat flow data along the fault. As discussed below, the direction of the maximum horizontal principal stress in the vicinity of an extremely weak fault must be either nearly perpendicular or parallel to the fault to minimize resolved shear stresses on the fault plane. Consistent with the argument that the low strength of the fault may be controlling crustal stress orientations is the observation that the direction of the maximum principal stress seems to rotate as the fault rotates in the big bend region of the fault (Fig. 1). Folds along the west side of the Great Central Valley that are subparallel to the San Andreas in central California bend and remain subparallel to the San Andreas as the fault begins to bend to the northwest of the Garlock fault in the southern San Joaquin Valley (*38*). Thus the stress orientation data suggest that the strength of the fault controls the orientation of the stress field and not the relative motion direction (~N35°W) of the Pacific and North American plates (*39–41*). One could argue that as the Fort Tejon (1857, M ~ 8.3) earthquake broke all the way from Parkfield (at the latitude of Coalinga) to Wrightwood (about 20 km northwest of Cajon Pass) with essentially pure right-lateral strike-slip motion despite a ~30° bend in fault strike (*42*), the sense of slip on the fault was controlled by the orientation of the weak fault and not some relatively uniform far-field driving stresses. Also, the stress field is essentially normal to the fault along the creeping section of the fault in central California (which does not sustain major earthquakes) and along the sections of the fault that broke in the 1906 San Francisco earthquake and the northern section of the Fort Tejon earthquake.

State of stress in southern California. The state of stress in southern California appears to be somewhat more complex than in central California. Any clear difference in tectonic style between eastern and western California south of the Garlock fault is unclear and some variability of the stress field along the strike of the San Andreas seems to be observed. Breakouts and focal mechanism data near the coast appear to show compression nearly perpendicular to the local trend of the San Andreas, similar to what is observed in central California. The P-axes of earthquake focal mechanisms in the southern Mojave Desert–eastern Transverse Ranges show compression at about N25°E, almost perpendicular to the strike of the San Andreas as in central California (*43*). To the northwest along the San Andreas in southern California, inversions of focal mechanisms for clusters of earthquakes within 10 km of the fault generally yield maximum horizontal compressive stress directions that are oriented ~55° to 60° to the strike of the fault (*44*).

Hydraulic fracturing stress measurements at ~2-km depth in the Cajon Pass research well show that the difference between the maximum and minimum horizontal principal stresses is only about 15 MPa, thus limiting the maximum horizontal shear stress acting on any vertical fault plane to only about 7.5 MPa (*45*). This is a factor of 2 to 3 lower than the shear stress levels predicted by frictional theory and extrapolation of the nearby in situ stress data at depths less than 1 km in the western Mojave. More important, the wellbore breakout and hydraulic fracture data on the orientation of the maximum horizontal principal stress in the Cajon Pass well indicate a complete lack of right-lateral shear stress at ~2-km depth (*45, 46*). Between depths of 1.7 and 2.1 km, approximately 80 distinct wellbore breakouts and two hydraulic fracture orientations indicate that the maximum horizontal stress is oriented about N70°E (*46*), 125° clockwise to the ~N55°W trend of the San Andreas in this region. This stress direction results in a small amount of left-lateral horizontal shear stress on planes parallel to the San Andreas.

Although the data on stress orientation at Cajon Pass are incompatible with right-lateral slip on the San Andreas fault, they are, however, fairly consistent with the local geology (*47*). Located only a few kilometers from the Cajon Pass drill site, the Cleghorn fault is characterized by Holocene left-lateral and normal fault slip (*47*). The fault strike and sense of movement are compatible with both the average stress orientation observed in the Cajon Pass borehole, as well as with stress magnitude data, which indicate a normal faulting stress state at ~1-km depth, that becomes a strike-slip stress-state at depths below ~1.5 km (*45*).

The stress measurements to be made in the Cajon Pass well at greater depth are critical to fully understand the local stress field and to assess the extent to which the shallow stress field is controlled by nearby faults (such as the Cleghorn) and not by the San Andreas

itself. Neither the stress data from the Cajon Pass well, nor the local geology around the site, is consistent with the ~N10°W to N20°W horizontal compressive direction indicated by regionally averaged earthquake focal mechanism inversion in the Cajon Pass region (*44*). Comparison of the Cajon Pass data with shallower in situ stress measurements in the area is also equivocal. The measurements near the San Andreas about 40 km to the northwest (*12*) have a maximum stress orientation of about N20°W, a value inconsistent with the Cajon Pass data. However, the maximum horizontal stress orientation measured in another borehole about equidistant from Cajon Pass, but further from the San Andreas (*48*), is consistent with the Cajon Pass measurements. Although the Cajon Pass data show some variability (in several short sections of the hole breakout, orientations differ from the median value by as much as ±30°, possibly because of localized effects of rock anisotropy), regardless of this variability, the data show a complete absence of right-lateral shearing stresses at ~2-km depth on planes parallel to the San Andreas.

Origin of fault-normal compression in central California. If the direction of relative motion between the North American and Pacific plates was highly oblique to the San Andreas, the observed direction of crustal compression in central California would not be surprising (*49*). However, the ~N35°W (*39–41*) relative plate motion direction and the ~N40°W fault strike in central California differ by ony about 5°, and it would seem that relative plate motion would result in essentially pure shear along the San Andreas and, in the context of classical faulting theory, an approximately north-south maximum compressive stress. As this is not observed, we briefly consider a simple model that is consistent with current estimates of relative motion between the North American and Pacific plates and that shows that an extremely weak fault can reorient far-field stresses. The model is based on the concept that shear stresses in the crust are high far from the fault and constrained by the frictional strength of the rock, but that shear stress on planes parallel to the "weak" faults of the San Andreas system must be quite low. Thus, the principal stresses must reorient themselves in order to minimize shear stress on the planes parallel to the San Andreas. This reorientation could result in either fault-normal compression or fault-normal extension.

If the San Andreas cannot withstand appreciable shear stress, equilibrium conditions require an increase in fault-parallel basal tractions acting on horizontal planes adjacent to the fault, which act to balance the decrease in shear parallel to the fault (*3*). The combined result of the decrease in shear stress parallel to the fault with the increase in basal shear stresses is to change the orientation of the stress field in the vicinity of the fault in two distinct ways. First, the direction of the maximum horizontal compressive stress in the far-field rotates to minimize the horizontal shear stress acting on the fault. As mentioned above, this rotation will be such that the direction of maximum principal stress becomes either nearly perpendicular or nearly parallel to the fault. The second change in the orientation of the stress field near the fault is due to the increase in basal shear. This results in a minor rotation of the vertical principal stress about the axis of the maximum principal stress.

To construct a simple model of the San Andreas fault to illustrate the principle of stress rotation, we must estimate both the orientation and magnitudes of the far-field stresses. For brevity, we apply this model only to central California, where the geometry of the San Andreas is quite simple and uniform fault-normal compression is observed. Let us first consider the orientation of far-field stresses. To the east of the San Andreas system, the direction of the maximum principal stress in the Sierra Nevada and Basin and Range provinces is about N10°E to N20°E (*18*). To the west of the San Andreas system in the Pacific plate, the orientation of the principal stress field is not known. However, the notion that relative plate motion is generating pure right-lateral shear on a plane striking about N35°W would suggest a maximum principal stress oriented about 45° to the east, or about N10°E. Thus, if we assume a far-field maximum compressive stress orientation of N10°E to N20°E, the angle between the fault and the far-field maximum stress would be about 50° to 60° in central California, where the San Andreas strikes about N40°W.

Next we must make an assumption about average magnitudes of the far-field crustal stresses. For the calculations we present in Fig. 4, we have assumed that far-field stress conditions generally correspond to a strike-slip faulting domain (the vertical stress is the intermediate stress) and that maximum stress differences are slightly less than the frictional strength of the crust (*50*). The principle demonstrated in Fig. 4 is that if the far-field shear stresses are significantly greater than the shear strength of the fault, a reorientation of the stress field must occur near the fault to lower the resolved shear stress on the fault (*51*). The precise assumptions about the magnitudes of the far-field stresses are not important in these calculations. We have used a strike-slip stress regime in the far-field because it is geologically most reasonable. Earthquakes in the Sierra Nevadas indicate both strike-slip and normal faulting and the stress field in the Sierras seems transitional between the Basin and Range and San Andreas provinces (*17, 22*).

In Fig. 4 we show the near-field angle between the maximum principal stress and the San Andreas fault as a function of the angle between the far-field maximum horizontal stress and the San Andreas for different values of the shear strength of the fault. We have computed the near-field maximum principal stress orientation assuming that a low strength fault simply reduces the magnitude of shear stresses parallel to it but does not alter the mean compressive stress in the crust (*51*). So long as the shear strength of the fault is limited to about 10 to 15 MPa, the orientation of the maximum principal stress near the fault in central California should be approximately perpendicular to the fault, although the far-field stresses are oriented only 50° to 60° from the fault (Fig. 4). However, if the average fault strength is as large as 50 MPa, almost no change in the orientation of the far-field stresses occurs (*52*).

An interesting aspect of the calculations discussed in (*53*) is that the near-field direction of maximum horizontal compression becomes nearly perpendicular to the San Andreas as long as the direction of the far-field maximum compressive stress is greater than 45° to the fault. However, if the direction of the far-field maximum horizontal stress is less than 45° to the strike of the fault, the direction of maximum horizontal compression becomes nearly parallel to the fault in order to minimize the resolved shear stress that results in fault-normal extension. Although the current direction of relative plate motion in central California is about N35°W and results in a slight component of compression across the San Andreas, prior to 4 million years ago the relative plate motion was more westerly (about N56°W) and produced a component of extension across the fault (*40*). Thus, the ~20° clockwise change in relative plate motion 4 to 5 million years ago would have caused a ~90° change in stress direction and tectonic style within about 100 km of the San Andreas—from fault-parallel basin development and fault-normal extension, to the uplift and fault-normal compression observed today. Sedimentological data from offshore basins in California suggest an onset of convergence about 5.5 MPa (*54*).

The state of stress in the vicinity of frictionless cracks in plates for various boundary conditions can be modeled to show that stresses near the cracks must be either parallel or perpendicular to the crack (*55*). However, two important problems indicate that detailed modeling at this time would be premature. First, the three-dimensional geometry of the San Andreas at depth is not known, and it has

been suggested that on the scale of the lithospheric thickness, the locus of shear strain appreciably widens at depth (*56*). Second, the exact nature of the shear tractions adjacent to the fault is unknown, but the width of the zone in which near fault-normal compression is observed may be related to the width of the zone in which subhorizontal tractions and crustal decoupling are important (*3*). If simple two-dimensional crack modeling is applicable to the San Andreas, the width of the zone of stress rotation is on the order of the depth of the crack (*55*). Thus the ~100 km zone on either side of the fault in which near fault-normal compression occurs suggests that the San Andreas is anomalously weak over a depth roughly equivalent to the thickness of the entire lithosphere.

As mentioned above, the increase in basal shear on subhorizontal faults below the seismogenic zone causes a minor rotation of the vertical principal stress with depth. For the same stress magnitudes for the calculations presented in Fig. 4 and an average level of shear stress on the San Andreas of 10 MPa, the intermediate principal stress would only deviate from the vertical by ~10° at a depth of 16 km (*57*).

Constitutive properties of a weak fault zone. The composition of the seismogenic portion of the San Andreas fault zone (upper ~15 km) is not known, but the fault zone does have a distinct geophysical signature with respect to surrounding rocks. A number of seismic, resistivity, and gravity studies have been performed that suggest that the San Andreas fault zone has very low seismic velocity, density, and resistivity (*58*) which suggests that it is highly deformed and potentially overpressured. Two basic types of mechanisms could explain a very low shear strength for the San Andreas fault. An obvious mechanism for lowering fault strength is that it is overpressured, that is, the high fluid pressure in the fault zone lowers the effective normal stress across the fault and allows sliding at extremely low shear stresses (*59*). For the San Andreas, this could logically result from the combined effects of fault-normal compression, high compressibility of fault zone materials, and low permeability of fault gouge (*60*). Shear heating associated with faulting could cause pore pressure to rise at the time of an earthquake and result in transient weakening of the fault (*61*).

However, in light of the stress orientation data in central California, there is an important problem with the hypothesis that the fault zone is weak due to the presence of abnormally high fluid pressures. The magnitude of pore pressure in the fault can only reach the value of the least principal stress (or else natural hydraulic fracturing would occur). Thus, if the coefficient of friction of fault zone materials is relatively high and similar to that of intact rock (*62*), even if the pore pressure is as high as the minimum horizontal principal stress, fault slip cannot occur on the San Andreas in response to a maximum horizontal compressive stress that is nearly perpendicular to it, as observed in central California (*63*). Thus other mechanisms may be responsible for lowering fault strength, including the possibility that the fault zone has an extremely low yield stress and coefficient of friction (*64*). If the strength of this gouge zone is quite low, the factors that control the strength and constitutive properties of the fault zone materials must be understood to explain the processes associated with earthquake initiation and propagation.

Conclusion. The state of stress along much of the San Andreas fault is characterized by fault-normal compression. This stress field indicates that the magnitude of shear stresses on the fault are extremely low, consistent with the implications of heat flow data near the fault. Simple model calculations show that the observed stress field is also consistent with current estimates of the direction of relative plate motions as long as the shear strength of the fault is appreciably lower than the level of far-field shear stresses in the crust.

The San Andreas and its related faults seem to represent pronounced zones of weakness, possibly through the entire lithosphere, that localize deformation and reorient tectonic stresses. Such a concept would clearly have broad applicability to faulting in other environments, especially other major strike-slip faults and subduction zones. Direct measurements of in situ stress at hypocentral depths are needed to verify this hypothesis. Sampling of the fault zone itself will be required to understand the mechanisms controlling fault strength to predict likely fault zone behavior before and during major earthquakes.

REFERENCES AND NOTES

1. J. N. Brune *et al.*, *J. Geophys. Res.* **74**, 3821 (1969); T. L. Henyey and G. J. Wasserburg, *ibid.* **76**, 7924 (1971).
2. A. H. Lachenbruch and J. H. Sass, *Proceedings of the Conference on Tectonic Problems of the San Andreas Fault* (Stanford Univ. Press, Stanford, CA, 1973), pp. 192–205.
3. ———, *J. Geophys. Res.* **85**, 6185 (1980).
4. See the compilation of stress drops by T. C. Hanks, *Pure Appl. Geophys.* **115**, 441 (1977).
5. A discussion of shear-stress magnitudes at depth on strike-slip faults classical faulting theory [see (*6*)] and laboratory-derived coefficients of friction [such as those summarized by J. D. Byerlee, *Pure Appl. Geophys.* **116**, 615 (1978)] can be found in R. H. Sibson [*Nature (London)* **249**, 542 (1974)] and in (*7*).
6. E. M. Anderson, *The Dynamics of Faulting and Dyke Formation With Applications to Britain* (Oliver and Boyd, Edinburgh, ed. 2, 1951).
7. J. C. Jaeger and N. G. W. Cook, *Fundamentals of Rock Mechanics* (Metheun, London, 1969).
8. R. H. Sibson, *J. Geol. Soc. London* **140**, 741 (1983).
9. H. Jeffries [*The Earth* (Cambridge Univ. Press, Cambridge, 1959), p. 195], showed that shear stress magnitudes beneath high mountain belts must be on the order of 100 MPa regardless of whether the load was elastically or inelastically supported. Numerous studies of lithospheric flexure result in predictions of high shear stress in the lithosphere. See, for example, R. Walcott, *J. Geophys. Res.* **75**, 3941 (1970); A. B. Watts and M. Talwani, *Geophys. J. R. Astros. Soc.* **36**, 57 (1974); B. Parsons and P. Molnar, *ibid.* **45**, 707 (1976); M. McNutt and W. Menard, *Geophys J. R. Astron. Soc.* **71**, 363 (1982). Although such results depend on the assumed lithospheric rheology [see H.-P. Liu, *J. Geophys. Res.* **85**, 901 (1980); P. England and D. McKenzie, *Geophys J. R. Astron. Soc.* **73**, 523 (1983)] as long as the upper crust is considered to deform elastically, flexural studies predict that shear stresses exceed 100 MPa.
10. See reviews by S. Kirby [in *Contributions in Tectonophysics 1979–1982* (American Geophysical Union, Washington, DC, 1983), pp. 1458–1502] and M. McNutt [in *Contributions in Tectonophysics 1983–1986* (American Geophysical Union, Washington, DC, 1987), pp. 1245–1254].
11. See, for example, J. D. Byerlee and W. F. Brace, *J. Geophys. Res.* **73**, 6031 (1968) and J. H. Dieterich, in *Mechanical Behavior of Crustal Rocks* (American Geophysical Union, Washington, DC, 1981), pp. 103–120.
12. A review of in situ stress measurements at depth near a number of active faults is given by M. D. Zoback and J. H. Healy [*Ann. Geophys.* **1**, 689 (1985)] who discuss the manner in which the frictional strength of the fault seems to control the magnitude of near-field stresses. Stress measurements at depths up to 850 m near the San Andreas are discussed by M. D. Zoback *et al.* [*J. Geophys. Res.* **85**, 6157 (1980)] and A. McGarr *et al.* [*ibid.* **87**, 7797 (1982)] and are basically consistent with the stress magnitudes predicted by laboratory-derived coefficients of friction.
13. J. R. O'Neil and T. C. Hanks, *J. Geophys. Res.* **85**, 6286 (1980).
14. See discussion in T. C. Hanks and C. B. Raleigh, *ibid.*, p. 6083.
15. Drilling and scientific measurements began at Cajon Pass in early December 1986. The project involves about 40 scientists from over a dozen institutions who are addressing a wide range of scientific objectives. Drilling and down-hole measurements stopped at 2.1 km in late March 1986 and resumed in November 1987. Target depth of the hole is 5 km. The project is being drilled under the supervision of DOSECC, Inc., a nonprofit consortium of approximately 35 universities. Funding is provided by the National Science Foundation, with substantial indirect support from the U.S. Geological Survey.
16. H. Kanamori [*Phys. Earth Planet. Inter.* **77**, 531 (1980)] presents a conceptually similar stress model of the lithosphere in which shear stress magnitudes in the lithosphere are generally high but low along major plate bounding faults.
17. M. L. Zoback and M. D. Zoback, *Geol. Soc. Am. Mem.*, in press. See also M. L. Zoback and M. D. Zoback, *J. Geophys. Res.* **85**, 6113 (1980).
18. By convention the *P* and *T* axes of focal plane mechanisms bisect the dilatational and compressional quadrants (that is, at 45° to the nodal planes). However, as pointed out by D. P. McKenzie [*Bull. Seismol. Soc. Am.* **59**, 591 (1969)] and C. B. Raleigh *et al.* [in *Flow and Fracture of Rocks* (American Geophysical Union, Washington, DC, 1972)], the direction of maximum compression can deviate from the *P*-axis and the amount of deviation depends on the coefficient of friction.
19. Shallow stress measurements show that various factors such as atmospheric temperature, rock fabric, local topography, fracture, and microfracture patterns can dominate tectonic stress effects, especially in the upper few meters [see, overview by T. Engelder and M. L. Sbar, *J. Geophys. Res.* **89**, 9365 (1984) and accompanying papers].
20. V. S. Mount, unpublished results.
21. See D. I. Gough and J. S. Bell, *Can. J. Earth Sci.* **19**, 1958 (1982); M. D. Zoback *et al.*, *J. Geophys. Res.* **90**, 5523 (1985); R. A. Plumb and S. H. Hickman, *ibid.*. p. 5513; R. A. Plumb and J. W. Cox, *ibid.* **92**, 4805 (1987).

22. I. Wong and W. U. Savage, *Bull. Seismol. Soc. Am.* **73**, 797 (1983); J. P. Eaton, private communication; L. M. Jones and R. S. Dollar, *Bull. Seismol. Soc. Am.* **76**, 439 (1986).
23. T. Atwater, *Geol. Soc. Am. Bull.* **81**, 3513 (1970).
24. A. Cox and D. Engebretson, *Nature (London)* **313**, 472 (1985); F. F. Pollitz, *ibid.* **320**, 738 (1986).
25. B. Page, in *The Geotectonic Development of California* (Prentice-Hall, Englewood Cliffs, NJ, 1981), pp. 329–417; B. Page *et al.*, *Geol. Soc. Am. Bull.* **90**, 808 (1979).
26. C. M. Wentworth and M. D. Zoback, in *U.S. Geol. Surv. Prof. Pap.*, in press; J. S. Namson and T. L. Davis, unpublished results.
27. J. Eaton and M. Rymer, in *U.S. Geol. Surv. Prof. Pap.*, in press.
28. I. G. Wong, R. Ely, A. Kollman, unpublished results.
29. A. Aydin and B. Page, *Geol. Soc. Am. Bull.* **95**, 1303 (1984).
30. D. S. McCulloch, in *Geology and Resource Potential to the Continental Margin of Western North America and Adjacent Ocean Basins—Beaufort Sea to Baja California*, D. W. Scholl, A. Grantz, J. G. Vedder, Eds. (Circumpacfic Council for Energy and Mineral Research, Earth Science Series, Houston, 1987).
31. E. Vittori, in *83rd Annual Meeting of the Cordilleran Section of the Geological Society of America, Abstracts with Programs* (Geological Society of America, Boulder, CO, 1987), p. 460.
32. The map in Fig. 3 is redrawn after T. W. Dibblee, Jr., *U.S. Geol. Surv. Misc. Geol. Inv. Map I-757* (1973). The cross section is redrawn from unpublished sections, courtesy of H. C. Wagner and J. A. Bartow of the U.S. Geological Survey.
33. C. M. Poley *et al.*, in *83rd Annual Meeting of the Cordilleran Section of the Geological Society of America, Abstracts with Programs* (Geological Society of America, Boulder, CO, 1987), p. 440.
34. W. Ellsworth, *Bull. Seismol. Soc. Am.* **65**, 483 (1975).
35. J. Savage, *Annu. Rev. Earth Planet. Sci.* **11**, 11 (1983).
36. W. Prescott, *J. Geophys Res.* **86**, 6067 (1981).
37. In the Parkfield region of central California, a study by P. Segall and R. Harris [*Science* **233**, 1409 (1987) (that did not use the boundary condition minimizing fault-normal compression)] showed that appreciable fault-normal compressive strain (0.06 ppm/year) occurs in addition to the shear strain induced by fault motion at depth (0.2 ppm/year). This data set included geodetic data from three separate sources (U.S. Geological Survey trilateration data and trilateration data from California Division of Mines and Geology and California Division of Water Resources), which made the analysis prone to systematic error (J. Savage, personal communication). R. O. Burford [thesis, Stanford University (1967)] analyzed triangulation data from the U.S. Coast and Geodetic Survey during the interval from 1930 to 1951 and found somewhat weak evidence of compression oriented oblique to the fault in the region where the San Andreas and Calaveras faults diverge, as well as just south of Parkfield.
38. C. W. Jennings, *Geologic Map of California* (1977).
39. J. B. Minster and T. H. Jordan, *J. Geophys. Res.* **83**, 5331 (1978); *ibid.* **92**, 4798 (1987).
40. D. Engebretson *et al.*, *Geol. Soc. Am. Spec. Paper* **206** (1986).
41. C. DeMets *et al.*, *Geophys. Res. Lett.*, in press.
42. K. Sieh, *Bull. Seismol. Soc. Am.* **68**, 1421 (1978).
43. J. Sauber *et al.*, *Geophys. Res.* **91**, 12683 (1987); T. H. Webb and H. Kanamori, *Bull. Seismol. Soc. Am.* **75**, 737 (1985). A compilation of earthquake focal mechanisms in southern California (for events in the past decade) has also been published by J. Pechman, thesis, California Institute of Technology (1985).
44. L. M. Jones, unpublished results, presents inversions of earthquake focal mechanisms for events within 10 km of the San Andreas along different sections of the fault in southern California. As the directions of maximum compression resulting from these inversions averaged 60° to 70° to the San Andreas, she argues that the fault must be moving with little resolved shear stress.
45. Preliminary stress measurements to ~2 km depth in the Cajon Pass borehole are described by J. H. Healy and M. D. Zoback, *Eos*, in press. Measurements to a depth of ~1.5 km in another well at the same location have been described by J. H. Healy and M. D. Zoback, *ibid.* **67**, 380 (1986).
46. The observations of hydraulic fracture and wellbore breakout orientations in the Cajon Pass well were obtained with a borehole televiewer, an acoustic scanning device described by J. Zemanek *et al.*, *Geophysics* **35**, 254 (1972). Three different, independently calibrated, televiewers were used to acquire the data and, in part, corroborated by a fourth magnetically oriented instrument of a different kind. The breakout data are summarized by G. Shamir and J. E. Springer, *Eos*, in press. C. Barton contributed substantially to the televiewer data processing.
47. R. Weldon, thesis, California Institute of Technology (1986).
48. J. M. Stock *et al.*, *Eos* **67**, 382 (1986).
49. See, for example, a discussion of highly oblique subduction by T. J. Fitch, *J. Geophys. Res.* **77**, 4432 (1987).
50. For the computations presented in Fig. 4, we used effective of 68, 136, and 204 MPa for the least, intermediate (vertical), and greatest effective principal stress at great distance from the San Andreas. Based on the assumption of hydrostatic pore pressure in the crust, these values correspond to an approximate state of stress at 8 km in a strike-slip faulting region (*5*) and is assumed to be roughly equivalent to the average stresses in the upper (seismogenic) part of the upper crust. These stress differences are conservative, that is, the difference between the horizontal stresses will not cause frictional sliding. Larger far-field shear stresses could have been used in these calculations, which would have emphasized even more the change in stress orientation shown in Fig. 4.
51. The calculations presented in Fig. 4 can be derived with a two-dimensional Mohr construction (*7*). If an initial stress state oriented such that the maximum principal stress is at an angle β to the fault, by reducing the shear stress parallel to the fault and by keeping the mean horizontal stress constant, a new orientation of the maximum principal stress α results and is given by

$$\alpha = \pi/2 - \tfrac{1}{2} \tan^{-1}\{2\, C_0[(\sigma_{Hmax} - \sigma_{hmin}) \cos(\pi - 2\beta)]\}$$

for $\beta > 45°$, where σ_{Hmax} and σ_{hmin} are the magnitudes of the maximum and minimum effective horizontal stresses and C_0 is the shear strength of the fault. For $\beta < 45°$

$$\alpha = \tfrac{1}{2} \tan^{-1}\{2\, C_0/[(\sigma_{Hmax} - \sigma_{hmin}) \cos(2\beta)]\}$$

As no change in stress orientation is necessary if the orientation of the far-field stresses results in little applied shear on the San Andreas, these equations are only valid when $\beta > \tfrac{1}{2} \sin^{-1}[2\, C_0/(\sigma_{Hmax} - \sigma_{hmin})]$ and $\beta < \pi/2 - \tfrac{1}{2} \sin^{-1}[2\, C_0/(\sigma_{Hmax} - \sigma_{hmin})]$. For the cases of interest (when C_0 is much less than $\sigma_{Hmax} - \sigma_{hmin}$), no change in stress orientation is required if the far-field direction of maximum horizontal compression is within a few degrees of being parallel or perpendicular to the fault.
52. Based on the stress orientations in central California alluded to in (*20*), V. S. Mount and J. Suppe (*Geology*, in press) use a two-dimensional Mohr construction to calculate large magnitude deviatoric stresses in the crust adjacent to the San Andreas (~100 MPa) by limiting the amount of shear stress on the fault to 10 to 20 MPa as indicated by the heat flow data and by considering the angle between the direction of maximum horizontal compression and the fault.
53. From the equations in (*51*), when $\beta < 45°$, $\alpha < \beta$, which resulted in a maximum horizontal stress almost parallel to the fault, and when $\beta > 45°$, $\alpha > \beta$ which resulted in near fault-normal compression.
54. J. K. Crouch *et al.*, in *Tectonics and Sedimentation along the California Margin*, J. K. Crouch and S. B. Bachman, Eds. (Pacific Section of the Society of Economists, Paleontologists and Mineralogists, Los Angeles, 1984), pp. 37–54.
55. See, for example, changes in stress direction in the vicinity of frictionless cracks in R. Dyer [thesis, Stanford University (1983)] and D. Pollard and P. Segall (unpublished results).
56. For an example, see (*8*).
57. It was shown in (*2*) that if the San Andreas fault is quite weak, the difference between the average shear stress parallel to the fault in the far field and that on the fault plane, $\Delta\tau$, is balanced by an increase in average shear stress on subhorizontal planes, τ_h, adjacent to the fault. The equations of equilibrium indicate that $\tau_h = (2D/W)\Delta\tau$ where D is the depth of the brittle, seismogenic part of the crust and W is the total width of the zone adjacent to the fault affected by the fault zone weakening and in which the basal shear acts. If we take D as ~15 km, the average depth of seismicity along the fault, W to be ~200 km [~100 km on either side of the fault (Fig. 1)], and $\Delta\tau \approx 40$ MPa, then $\tau_h \approx 6$ MPa. The result of nonzero τ_h near the fault at depth is to rotate the principal stress that is vertical near the surface (where $\tau_h = 0$) about the axis of the greatest horizontal principal stress. In the case of central California where the maximum principal stress is almost perpendicular to the San Andreas, the amount of rotation of the near-vertical principal stress at about 16 km is less than 10° because the magnitude of τ_h is so much less than the magnitudes of the vertical stress and the minimum horizontal principal stress.
58. R. Feng and T. V. McEvilly, *Bull. Seismol. Soc. Am.* **73**, 1701 (1983); W. D. Mooney and R. Colburn, *ibid.* **75**, 175 (1985); C.-Y. Wang, *J. Geophys. Res.* **89**, 5858 (1984); A. M. Trehu and W. H. Wheeler IV, *Geology* **15**, 254 (1987).
59. M. K. Hubbert and D. Rubey [*Geol. Soc. Am. Bull.* **70**, 115 (1959)] showed that the shear stress required to move faults can be dramatically reduced by reducing the effective normal stress (the normal stress minus the pore pressure) acting on a fault plane by increases in pore pressure.
60. C. Morrow *et al.*, *Geophys. Res. Lett.* **8**, 325 (1981).
61. A. Lachenbruch, *J. Geophys. Res.* **85**, 6097 (1980); C. B. Raleigh and J. Evernden, in *Mechanical Behavior of Crustal Rocks* (American Geophysical Union, Washington, DC, 1981). J. Melosh, *Geophys. Res. Lett.* **5**, 321 (1978) has suggested an "acoustic fluidization" mechanism for transient fault zone weakening.
62. Friction experiments of blocks of rock separated by a layer of dry fault gouge by R. Summers and J. D. Byerlee [*Int. J. Rock Mech. Miner. Sci.* **14**, 155 (1977)] show friction values that increase with total strain and suggest that at high strains the frictional strength of the gouge would be consistent with the relatively high friction of intact rocks.
63. A simple Mohr-Coulomb construction can be used to show that when the pore pressure is equal to the value of the minimum horizontal stress, faulting cannot occur if the angle between the fault normal and the maximum principal stress θ is less than the angle of friction φ. For coefficients of friction of 0.6 and larger (*62*), φ is greater than 30°. Thus, in central California where the angle θ is only on the order of 10° to 20°, high pore pressure in the fault zone is not sufficient to permit faulting.
64. C.-Y. Wang *et al.*, *J. Geophys. Res.* **85**, 1462 (1980); C.-Y. Wang and N. Mao, *Geophys. Res. Lett.* **6**, 825 (1979). The difference between these results and those of (*62*) and the exact role of pore fluid in the deformation process is not known.
65. We thank A. Lachenbruch, J. Savage, R. Weldon, A. McGarr, and an anonymous reviewer for comments on earlier versions of this manuscript and for suggesting important improvements.

27 July 1987; accepted 5 October 1987